Viral metagenomic analysis of the cheese surface: a comparative study of rapid procedures for extracting virus-like particles

Eric Dugat-Bony, [a]# Julien Lossouarn,[b] Marianne De Paepe,[b] Anne-Sophie Sarthou,[a] Yasmina Fedala,[c] Marie-Agnès Petit,[b] and Stéphane Chaillou[b]

[a]UMR782 GMPA, INRA, AgroParisTech, Université Paris-Saclay, Avenue Lucien Brétignières, 78850, Thiverval-Grignon, France

[b]UMR1319 MICALIS, INRA, AgroParisTech, Université Paris-Saclay, Domaine de Vilvert, 78350, Jouy-en-Josas, France

[c]Institut Langevin, ESPCI Paris, CNRS, PSL University, 1 rue Jussieu, 75005 Paris, France

Running Head: Viral extraction procedure for cheese virome analysis

#Address correspondence to Eric Dugat-Bony, eric.dugat-bony@inra.fr

KEYWORDS

Cheese rind, viral metagenomic, VLPs extraction procedure

ABSTRACT

The structure and functioning of microbial communities from fermented foods, including cheese, have been extensively studied during the past decade. However, there is still a lack of information about both the occurrence and the role of viruses in modulating the function of this type of spatially structured and solid ecosystems. Viral metagenomics was recently applied to a wide variety of environmental samples and standardized procedures for recovering virus-like particles from different type of materials has emerged. In this study, we adapted a procedure originally developed to extract viruses from fecal samples, in order to enable efficient virome analysis of cheese surface. We tested and validated the positive impact of both addition of a filtration step prior to virus concentration and substitution of purification by density gradient ultracentrifugation by a simple chloroform treatment to eliminate membrane vesicles. Viral DNA extracted from the several procedures, as well as a vesicle sample, were sequenced using Illumina paired-end MiSeq technology and the subsequent clusters assembled from the virome were analyzed to assess those belonging to putative phages, plasmid-derived DNA, or even from bacterial chromosomal DNA. The best procedure was then chosen, and used to describe the Epoisses cheese virome. This study provides the basis of future investigations regarding the ecological importance of viruses in cheese microbial ecosystems.

IMPORTANCE

Whether bacterial viruses (phages) are necessary or not to maintain food ecosystem function is not clear. They could play a negative role by killing cornerstone species that are necessary for fermentation. But they might also be positive players, by preventing the overgrowth of unwanted species (*e.g.* food spoilers). To assess phages contribution to food ecosystem functioning, it is essential to set up efficient procedures for extracting viral particles in solid

44 food matrix, then selectively sequence their DNA without being contaminated by bacterial
45 DNA, and finally to find strategies to assemble their genome out of metagenomic sequences.
46 This study, using cheese rind surface as a model, describes a comparative analysis of
47 procedures for selectively extracting viral DNA from cheese and to efficiently characterize
48 the genome of dominant phages with cross-sample assembly.

INTRODUCTION

The cheese surface hosts dense and diverse microbial communities composed of bacteria, yeasts and filamentous fungi. Composition of these communities has been studied for decades (see (1) and (2) for reviews). With the help of high throughput sequencing techniques, we now have detailed pictures of the communities present in a large panel of cheese varieties, and from all over the world (3–6). However, like many other microbial ecosystems, there is still a lack of knowledge on whether and how viral diversity controls the structure of cheese surface microbiota.

Viruses infect all forms of life (7), from prokaryotes (8) to eukaryotes (9) and, in some particular cases, viruses themselves (10). In microbial ecosystems, viral predation is known to greatly influence the structure and functioning of microbial communities (11–13). Nevertheless, since virus genomes lack a single marker sequence for phylogenetic analysis, the structure and role of viral communities in nature are rarely evaluated. Recently, viral shotgun metagenomics helped to describe viral communities from environmental samples including ocean, freshwater, soil, mammalian gut and, to a minor extent, fermented food products (14). Nevertheless, there is currently no literature on the viral diversity of the cheese surface.

Protocols for extraction of virus-like particles (VLPs) have been optimized for different environments (15–18). For food samples, most available procedures have been designed for the recovery of foodborne viruses potentially affecting human health such as noroviruses, rotaviruses (RoV) and hepatitis viruses (19), but not for microbial viruses such as bacteriophages. Furthermore, because the cheese surface has peculiar characteristics such as the presence of caseins at high concentration, high fat and salt content, it proves necessary to set up a dedicated procedure. Ideally, the method should be easy-to-use and rapid enough to

be compatible with medium (dozens to hundred samples) to large-scale studies (hundreds to thousands samples) such as those performed to describe microbial communities (6).

Taking into account all these constraints, we compared four procedures for the isolation of viruses from cheese surfaces. The backbone of the protocol followed the PEG-based protocol already evaluated by Castro-Mejia et al. on fecal samples (15). However, we replaced the buffer used for sample suspension, and tested both the effect of adding a filtration step before PEG precipitation in order to completely remove microbial cells and the substitution of the expensive and time-consuming density gradients for VLPs purification by a simple chloroform treatment which is used for membrane vesicles removal (20, 21) (Fig. 1). We evaluated the usefulness of the four procedures for cheese virome analysis (limited to the viruses with DNA genomes, expectedly the most abundant) using three different types of cheese, namely Camembert, Epoisses and Saint-Nectaire, and following two criteria: particles recovery and particles purity. Finally, we assessed the level of microbial DNA contamination in virome sequencing data for one type of cheese.

RESULTS

Quantification and purity of VLPs recovered from the cheese surface.

Among the four tested procedures, only those containing chloroform treatments (P2 and P4) resulted in VLP solutions sufficiently pure to allow nanoparticle counting using the interferometric light microscope (Table 1). We observed 1×10^9 to 4×10^{10} nanoparticles per gram of cheese surface, and filtration did not induce a drastic loss of particles. Counts were higher in Epoisses and Camembert than in Saint-Nectaire cheese. Camembert had the highest nanoparticles per microbial cell ratios. This type of cheese had the lowest bacterial counts (Table S1), whether such a community leads to higher cell lysis mediated by viruses or higher levels of membrane vesicles remains to be investigated. VLP solutions prepared using

procedures P1 and P3, without chloroform treatment, were very dense, milk-white and led to hard noise in interferometer's films with a myriad of spots larger than those typically observed for viruses. Microbial cells clearly contaminated the VLP fractions when using procedures P1 and P2, without filtration (Table 1, column 3). It has to be mentioned we also observed bacterial cells in one filtrated sample, *i.e.* Camembert cheese with P3, indicating probable post-filtration contamination.

Two-layer iodixanol gradients were used as quality controls in order to separate microbial cells, debris and membrane vesicles from viruses, enabling to visually observe the effect of the four procedures on the quantity and purity of VLP solutions (Fig. 2). For the three types of cheese tested, similar profiles were observed after ultracentrifugation. A strong band located at the top of the lightest density layer was present in samples prepared without filtration and chloroform treatment (P1) suggesting high contamination with microbial cells, debris and membrane vesicles (Fig. 2, red arrow). This band was still present – albeit slightly less intense – in filtered samples (P3), suggesting that cheese rind is rich in membrane vesicles. Finally, this band was completely absent from samples prepared with procedures including chloroform treatment (P2 and P4) confirming the efficiency of such treatment for removing membrane vesicles from VLP solutions (20). A visible band containing viruses formed at the proximity of the 45% iodixanol cushion (Fig. 2, blue arrow), at a density corresponding to 40% iodixanol, as estimated with a refractometer. This virus band was barely visible, however, in samples treated with chloroform (P2 and P4) when compared to untreated samples (P1 and P3). Nanoparticles quantification using interferometry in the viral band of Epoisses samples after dialysis indicated that samples treated with cholorofom (P2 and P4) contained approximately ten times less nanoparticles than untreated samples (P1 and P3). For Camembert cheese and procedure P3, we observed two distinct bands near the 45% iodixanol

cushion. Transmission electronic microscopy revealed that viruses were more abundant in the lowest one.

Altogether, these results suggest that filtration is an essential step in cheese VLPs preparation in order to completely eliminate microbial cells, which represent the major source of DNA contamination in virome studies. Furthermore, chloroform treatment is very beneficial for VLP solutions' cleaning and removal of membrane vesicles, which might contain pieces of microbial DNA (see below), but at the cost of reducing the nanoparticle recovery.

Effect of the extraction procedure on the composition of the Epoisses virome

Saint-Nectaire exhibited the lowest nanoparticles per cell ratio and Camembert the highest, Epoisses being an intermediate situation (Table 1). Furthermore, plate counting indicated a higher bacterial density in Epoisses cheese than in Camembert (Table S1), bacteria being expected as the main targets of microbial viruses (bacteriophages or phages) in the cheese ecosystem. For those two reasons, we selected Epoisses cheese as the best candidate for further virome analysis. DNA was successfully extracted from VLP solutions produced from Epoisses cheese using the four procedures and prior the gradient step. DNA yields are available in Table S2. DNA samples were then sequenced, in order to assess the impact of both filtration and chloroform treatment on the final sequence dataset (see Material and Methods section). In addition, for sample P3, the vesicle band was recovered from iodixanol gradient, DNA was extracted using the same protocol as viruses, and sequenced. The virome sequence data from each of the 12 samples (4 protocols x 3 biological replicates) and that of the vesicles sample were binned together for assembly of the virome (see Material and Methods section for more details).

Quality filtered reads were pooled and assembled into 910 contigs of length greater than 2,500 bp, a threshold used for keeping putative small virus genomes (22). Of these, 124 contigs were selected for further analysis based on VirSorter results and coverage criteria (see

147 Material and Methods section). These 124 contigs were ranging in size from 2.5 kb to 122 kb
148 with a N50 of 24.4 kb and were designated as the Epoisses cheese virome. Mapping of the
149 quality filtered reads against this virome revealed that microbial cell contamination was
150 higher with protocol P1 and in the vesicles sample than in any of the other three protocols
151 (Fig. 3).
152 The contigs were further analyzed and separated into four classes based on PHASTER and
153 Blast results (*i.e.* probable phage contigs, plasmid-derived contigs, putative plasmid-derived
154 contigs and unclassified contigs) (Dataset S1). Principal coordinate analysis performed on the
155 Bray-Curtis dissimilarity index calculated from the abundance table of the 124 contigs (Fig.
156 4A) showed an ordination of the samples according to the VLP extraction procedure, with
157 samples obtained with P1 and P3 being separated from samples obtained with P2 and P4. This
158 indicated a possible impact of the chloroform treatment on the quality of the resulting virome.
159 Datasets produced with protocols P2, P3 and P4 were strikingly enriched for reads mapping to
160 probable phage contigs (>99% in average) when compared to VLP fraction obtained with P1
161 (94% in average) (Fig. 4B), which was largely explained by the higher proportion of
162 unmapped reads present in P1 samples (Fig. 4F). The relative proportion of reads mapping to
163 the 19 plasmid-derived contigs was greatly reduced in samples treated with P3 (filtration) and
164 even more so in samples treated with P2 (chloroform) and P4 (chloroform and filtration),
165 when compared to P1 (Fig. 4C), reflecting the positive impact of both filtration and
166 chloroform treatment on the quality of the final virome. The relative proportions of reads
167 matching putative plasmid-derived contigs (Fig. 4D) and unclassified contigs (Fig. 4E)
168 remained similar regardless of the VLP extraction procedure.
169 Detailing the composition of each virome evidenced that the detection of contigs identified as
170 probable phages was not affected by the VLP extraction procedure (Fig. 5), suggesting that
171 neither the filtration step nor the chloroform treatment biased the sample composition. The

major differences were observed for the 39 contigs belonging to the categories plasmid and putative plasmid. Most of them were undetected or sporadically detected in samples treated with chloroform (P2, P4). They were on the contrary much higher with protocols P1 (and to a lesser extend P3) and highly abundant in the vesicles sample (39% of the reads). Interestingly, NODE-134, the most abundant contig detected in the vesicles sample (24 % relative abundance) and assigned to the plasmid-derived contig category, was only marginally detected in samples treated with protocols P1, P2, P3 and P4 (<0.005% relative abundance).

Composition of the Epoisses cheese virome

Three repeats of the extraction-sequencing on Epoisses cheese bought simultaneously from the same manufacturer gave highly reproducible results. Two contigs, NODE-1 and NODE-4, now named Epvir4 and 949_Epvir1, were prevalent, representing relative mean abundances of 63% and 28%, respectively. Epvir4 genome is 42 kb long. It was assigned by VirSorter as a category 2 phage (« quite sure ») but did not share similarity with already known phages. The annotation by RAST, HHpred and BLAST revealed an organization into functional modules (Fig. S1A). Amongst the ORFs with predicted homologues in nr database, most best BlastP matches (63%) were found in the genus *Glutamicibacter* (formerly *Arthrobacter*) suggesting that the host of this abundant phage might be a *Glutamicibacter* species (Dataset S2). 949_Epvir1 genome (Fig. S1B) is 122 kb long and shares 95% nucleotide identity and 95% coverage with *Lactococcus lactis* phage 949, a virulent phage (despite two predicted integrase genes) isolated from cheese whey in New Zealand (23). The third most abundant contig (1.1% of the reads), Epvir8, has a genome 41 kb in length, and shares a small 1.1 kb region with 88% nucleotide identity with *Pseudoalteromonas* phage SL25 (24). Amongst the ORFs with predicted homologues, more than half (56%) were found in *Pseudoalteromonas* phages while another quarter (24%) were found in *Vibrio* phages (Dataset S2 and Fig. S1C)). All other contigs exhibited a relative abundance lower than 1%, most of them being difficult to assign

to a putative host. Nevertheless, few contigs were closely related to *Lactococcus lactis* phages (*e.g.* NODE-15, NODE-59, NODE-142), *Pseudoalteromonas* phages (*e.g.* NODE-48, NODE-276), *Vibrio* phages (*e.g.* NODE-12, NODE-116), *Leuconostoc* phages (*e.g.* NODE-18, NODE-658) and *Halomonas* phage (NODE-636). All of these bacterial genera are frequently detected as part of cheese surface (3). The best assignments carried out for all contigs are available in supplementary Dataset S1.

DNA content of Epoisses membrane vesicles

Much less DNA was present in membrane vesicles, compared to total viromes (Table S2). This has to be kept in mind when comparing the vesicle line to the virome lines in Fig. 5, since colors reflect only relative abundances. Almost 51% of the reads from the vesicles sample mapped to contigs assigned to potential phages, which indicated that phage DNA was present in the vesicles. Interestingly, the reads corresponding to plasmid-derived contigs were specifically enriched in membrane vesicles (10% of total), relative to the viromes (0.03%). It seems therefore that the plasmid content of samples P1 and P3, observed in Fig. 5, originate from membrane vesicles, which are still present since no chloroform treatment was applied in these protocols. The total DNA content obtained from the vesicles fraction was low, relative to viromes, with only 3.8 ng (Table S2), and corresponded to an estimated amount of 1.3×10^{11} nanoparticles according to interferometry measures. Supposing all DNA content is plasmidic, with an average size of 5 kb for the plasmids (and a corresponding weight of 0.55 x 10^{-17} g), 3.8 ng of DNA would amount to 7×10^{8} plasmidic DNA molecules, suggesting that only 0.5% of the vesicules effectively contain a DNA molecule. The same calculation for phage DNA (~50 kb) would result in 10-fold less DNA containing membrane vesicles.

DISCUSSION

With the increasing attraction for virome sequencing, protocols for extracting viruses from diverse environmental samples have been developed during the past decade. Prior to nucleic acid extraction and sequencing, these protocols usually included sample pretreatment to make viral particles accessible for extraction, virus concentration and finally virus purification (18). Each step has to be adapted, according to the type of samples studied and the type of virus targeted. For cheese, we chose to blend the samples after a dilution step in trisodium citrate, in order to maximize the chance for recovering viral particles from the matrix. Indeed, citrate is a complexing agent for calcium and allows casein solubilization. It is largely used in nucleic acid extraction protocols for recovering microbial cells from casein network in milk and cheese (25, 26).

We also decided to evaluate the potential benefit of adding a filtration step (0.22 µm) on the quality of VLPs preparation and of the resulting virome. Filtration is generally avoided in virus extraction protocols from environmental sources because some viruses can be very large, even larger than microbial cells (27). Nevertheless, our choice was motivated by the fact that (i) such large viruses are generally hosted by organisms which are not part of the cheese ecosystem such as amoebas, protists and microalgae (ii) it ensures complete removal of microbial cells which generally account for the major source of contaminating DNA sequences in virome studies (28). Our results demonstrated that adding filtration to the extraction procedure reduced microbial contamination of the cheese VLP solutions by microbial cells, without major modification neither in the particle counts nor in the final virome profile.

The best way to purify VLP includes a density gradient ultracentrifugation step (18), in which viruses are separated from other components of the extract based on their physical properties. This technique is, however, very time-consuming, expensive and requires specific technical skills and lab equipments. Chloroform treatment represents a possible alternative for rapid

and efficient virus purification (20, 29) and has already been used in the viral metagenomic context (30). This solvent permeabilizes the membranes of bacterial cells and membrane vesicles, disrupting their structural integrity and making nucleic acids available for digestion by nucleases. Our results indicate that such treatment, in combination with filtration, is mandatory for successful quantification of VLP extracted from cheese samples by interferometry. Even if viral capsids are said to be resistant to chloroform (20, 31), it is important to mention that some viruses, in particular enveloped viruses, might be lost after such treatment (18, 20, 21, 32). Comparing the Epoisses cheese VLP solutions obtained with procedures including chloroform treatment or not, indicated a loss of VLP upon chloroform treatment (as illustrated in Fig. 2). Analyzing the nanoparticle counts in the viral band of one Epoisses cheese after density gradient ultracentrifugation and dialysis indicated that we recovered approximately ten times less nanoparticles in chloroform-treated samples versus non-treated samples. However, this was accompanied by a limited reduction of the final DNA yields (<3 times less DNA in average for treated versus untreated samples, Table S2) and we did not observe qualitative differences in the abundances of viral contigs as a function of chloroform treatment. Furthermore, adding chloroform treatment to the extraction procedure resulted in a significant enrichment of the virome in actual viral sequences while drastically reducing the proportion of plasmids and sequences from microbial origin (unmapped reads).

For one Epoisses, sequencing of the DNA content of a membrane vesicle fraction, obtained after separation from phage particles on an analytical density gradient, was performed. A low amount of DNA was recovered, in comparison with total viromes, suggesting that at most a few percent of the membrane vesicles contain DNA. This is in line with the current view that the transport of nucleic acids only constitutes one of many potential roles for membrane vesicles. Membrane vesicles are involved in exchanges between cells in the tree domains of life (33). In the bacterial domain, they have multifaceted roles including the delivery of

autolysins, cytotoxins and virulence factors, as well as nucleic acids (34, 35). In our membrane vesicle sample, DNA sequencing leads us to formulate several suppositions: i) since half of vesicle reads map to contigs classified as potential phages, it may be that Epoisses membrane vesicles serve as decoys and trap phages, as recently reported in *Vibrio cholerae* (36). The interaction between phage tail fibers and membrane vesicles harboring proper phage receptors could contribute to the emptying, and thereby inactivating of phage virions, after DNA injection. ii) The enrichment in reads corresponding to predicted plasmids, compared to total viromes, suggests that Epoisses membrane vesicles transport plasmid DNA, as described for an *Escherichia coli* strain (37). iii) A third category of DNA content in this vesicle fraction, composed of circular contigs that might be plasmidic but with no hit in databases, might not belong to vesicles. Indeed, the relative proportions of these contigs are similar in each virome, irrespective of the chloroform treatment. These DNA fragments might be packaged by transducing phage particles, which are more resistant to chloroform than vesicles. One has to suppose that such transducing particles have a lower density than *bona fide* phage particles to explain their presence together with vesicles fraction.

The set up of the protocol most adapted to recover viral communities from cheese rind was considerably facilitated by the use of a microscopic device called interferometer, allowing evaluating in real time the total nanoparticle counts (38, 39). It permitted in particular to choose, among several cheeses, those with higher nanoparticle titers for the present study. Camembert and Epoisses cheeses had markedly more nanoparticles, compared to Saint-Nectaire (Table 1). Camembert and Epoisses cheese are both soft cheeses, characterized by a bloomy and washed rind, respectively. These types of cheese typically have a higher moisture content than semi-soft pressed cheese with natural rind such as Saint-Nectaire (40, 41). Although a more comprehensive comparison including more cheese varieties would be

295 required, our results are congruent with the general assumption that viruses would be more
296 abundant in hydrated environment, compared to dry ones.
297 The rapid procedure presented in this study enabled to obtain sufficient quantity of viral DNA
298 from Epoisses cheese (equivalent of 1.5 gram as starting material for each protocol) for direct
299 library preparation prior to sequencing, avoiding the use of multiple displacement
300 amplification (MDA) (DNA quantities obtained for all samples presented in this study are
301 available in Table S2). MDA is widely used in viral metagenomic studies due to the
302 insufficient DNA material extracted from the samples (18). However, amplification bias has
303 been documented for this technique (42) which might provoke distortion in the viral
304 community profiles and making preferable direct DNA sequencing when possible.
305 The Epoisses virome analyzed in this study was composed of many contigs sharing high
306 sequence identity with known *Lactococcus lactis* phages including the widely known 936,
307 P335 and C2-like groups. Interestingly, the second most abundant one (28% of reads), named
308 949_Epvir1, was very similar to the *L. lactis* phage 949, a virulent phage isolated from cheese
309 whey in New Zealand, which is phylogenetically distant from those groups of commonly
310 isolated *L. lactis* phages (23). *Lactococcus lactis* is used as starter in the manufacture of
311 Epoisses cheese. In a previous work describing the microbial diversity in twelve french
312 cheese varieties, it was detected as the dominant bacterial taxa in the core of Epoisses cheese
313 and was also highly detected in the rind (3). In the same study, other dominant bacterial
314 genera of the Epoisses cheese rind included not-deliberately inoculated taxa such as, by order
315 of importance, *Psychrobacter*, *Marinomonas*, *Vibrio*, *Pseudoalteromonas*, *Glutamicibacter*,
316 *Mesonia*, *Enterococcus*, *Lactobacillus* and *Halomonas*. Interestingly, phages potentially
317 infecting some of such non-starter bacterial taxa, including *Glutamicibacter* (Epvir4, most
318 abundant contig in the Epoisses virome, 63% of the reads), *Pseudoalteromonas* (Epvir8, third

most abundant contig, 1.1% of the reads), *Vibrio*, *Leuconostoc* and *Halomonas*, were also detected in the Epoisses cheese virome.

The cheese surface microbiota is in constant evolution during the ripening process, and is characterized by the successive development of different microbial groups. Microbial interactions between different species have been observed in cheese (43–46), providing the first elements of comprehension regarding biotic forces sustaining microbial assemblage in this peculiar environment. Our results indicate that many microbial species living on the cheese surface are also subjected to viral predation, and shed light on the need of careful evaluation of the impact of viruses on the dynamic of the cheese microbial ecosystem.

CONCLUSION

In this study, we optimized a rapid protocol for VLP extraction from the cheese matrix suitable for subsequent virome analysis. We demonstrated its efficiency by extracting VLPs from three different type of cheese and produced the first cheese surface virome using Epoisses cheese as a model. Our results emphasized the positive impact of both filtration and chloroform treatment on the final virome quality in the cheese context. In the future, we anticipate virome analysis will expand our knowledge on cheese microbial ecosystems and possibly give the opportunity to better understand the rules of microbial assembly that occur in this fermented food.

MATERIAL AND METHODS

Sampling procedure

Three types of French surface-ripened cheese were studied, namely Camembert (CAM, bloomy rind), Epoisses (EP, washed rind) and Saint-Nectaire (SN, natural rind). For each type of cheese, three cheeses produced at the same date and from a unique producer were

344 purchased and analyzed as replicates. Rind was gently separated from the core using sterile
345 knives, and mixed using a blender.

346 **Microbiological analysis**

347 One gram of the cheese surface was diluted 1:10 in sterile saline solution (9 g/l NaCl) and
348 homogenized with an Ultra Turrax Homogenizer (Labortechnik, Staufen,Germany) at full
349 speed for 1 min. Serial dilutions were performed in 9 g/l NaCl and microorganisms were
350 enumerated by surface plating in duplicate on specific agar base medium. Cheese-surface
351 bacteria were enumerated on brain heart infusion agar (Biokar Diagnostics) supplemented
352 with 22.5 mg/l amphotericin B after 3 to 5 days of incubation at 25°C under aerobic
353 conditions. Lactic acid bacteria were enumerated on de Man-Rogosa-Sharpeagar (pH 6.5,
354 Biokar Diagnostics) supplemented with 22.5 mg/l amphotericin B after 3 days of incubation
355 at 30°C under anaerobic conditions. Finally, fungal populations were enumerated on yeast
356 extract-glucose-chloramphenicol (Biokar Diagnostics) supplemented with 2,3,5-
357 triphenyltetrazolium chloride (10 mg/l) after 3 to 5 days of incubation at 25°C under aerobic
358 conditions.

359 **Extraction of virus-like particles (VLPs)**

360 Four protocols, named P1, P2, P3 and P4, were tested in parallel starting from the same
361 material (Fig. 1). Six grams of cheese rind was diluted 1:10 with cold trisodium citrate (2%
362 w/v) into a sterile bag and mixed for 1 min using a BagMixer (Interscience). Citrate is a
363 complexing agent for calcium and allows casein solubilization. It is largely used in nucleic
364 acid extraction protocols for recovering microbial cells from casein network in milk and
365 cheese (25, 26). The solution was centrifuged at 300 × g for 10 min at 4°C in order to pellet
366 big aggregates. The supernatant was centrifuged at 5,000 × g for 45 min at 4°C in order to
367 pellet microbial cells. At this stage, the supernatant containing free VLPs was diluted 1:5 with
368 cold SM buffer (200 mM NaCl, 10 mM $MgSO_4$, 50 mM Tris pH 7.5) and split, half being

used for filtration-free protocols (protocols P1 and P2) and half being successively filtrated using 0.45µm and 0.2µm polyethersulfone membranes and glass vacuum filter holders (Millipore) (protocols P3 and P4). Samples, filtrated or not, were then supplemented with 10% PEG 6,000 (Sigma) and kept at 4°C over-night after dissolution for VLPs precipitation. After centrifugation at 6,000 × g for 1h at 4°C, pellets were resuspended with 2 ml of cold SM buffer and split again, half being stocked at 4°C (protocols P1 and P3) and half being treated with chloroform in order to eliminate membrane vesicles (protocols P2 and P4). More specifically, 1 volume of fresh, non-oxidized chloroform was added to the sample and mixed thoroughly for 1 min using a vortex to create an emulsion. After centrifugation at 15,000 × g for 5 min at 4°C, the aqueous phase containing viral particles was recovered.

Particles counting using Interferometry

A "home-made" interferometric light microscope (ILM) (38) was used to count nanoparticles (i.e. both vesicles and viruses) present in our VLP fractions as previously described (39). Briefly, 5 µl of each sample were used to collect a stack of 200 images (CMOS camera). We developed a simple ImageJ (47) script that allows first background subtraction and image quality enhancement, then particles localization on each image. An average number of nanoparticles per frame was obtained. To calibrate the concentration estimates, crude lysates of phages P1, T4, T5, T7, λCI857 and φX174 were titrated on *Escherichia coli* MG1655, and counted with the ILM device. These counts were converted into concentrations, assuming that all particles present in the observation volume (10^{-8} ml) were detected with the ILM device. Table S3 and Fig. S2 showed a good match between the two measurements, usually within a +/- 3 fold range for phages P1, T4, T5, T7 and λCI857, whereas φX174 was underestimated by 20 fold. We next compared the ILM estimates with epifluorescence microscopy on two VLP samples obtained from Epoisses cheese (Fig. S3). As shown in the result section, virome samples of Epoisses rind also contain vesicles, which are detected by ILM, but not by

394 epifluorescence, since they mostly do not contain DNA. In accordance with expectations, 1.5
395 to 1.9-fold more particles were counted by ILM than by epifluorescence. We concluded that
396 the ILM measurements give reasonable estimates of nanoparticle concentrations (both
397 vesicles and VLP) of viromes.

398 **Particles purity evaluation using iodixanol gradients**

399 Two-layer iodixanol discontinuous gradients of 45% and 20% (w/v) in SM Buffer (50 mM
400 Tris pH7.5, 100 mM NaCl, 10 mM MgCl2) were prepared by adding first 6 ml of the 20%
401 fraction in a 12 ml ultracentifugation tube, and then under layering 4.5 ml of the 45% fraction
402 in the bottom of the tube, using a glass transfer pipette and a pipette pump. Each VLP solution
403 (1 ml diluted 1:2 with SM Buffer) was finally added on top of the gradient and the tubes were
404 centrifuged at 200,000 × g for 5 h at 10°C, in an SW41 rotor, using a Beckman XL-90
405 ultracentrifuge.

406 **Viral DNA extraction**

407 500 µl of the VLPs preparation were treated for 30 min at 37°C with 1 U of TURBO DNase
408 (Invitrogen) in order to digest free DNA. DNase was inactivated by the addition of 5.5 µl of
409 100 mM EDTA and the sample was placed on ice for 5 min. The entire content of the tube
410 was transferred to a 2 ml tube containing a gel that improves separation between the aqueous
411 and organic phases (Phase Lock Gel Heavy; Eppendorf AG, Hamburg, Germany). One
412 volume of phenol-chloroform (1:1; saturated with 10 mM Tris pH 8.0, and 1 mM EDTA) was
413 added to the sample and, after gentle mixing for 1 min by inversion, the tube was centrifuged
414 at 10,000 × g for 10 min at 4°C.The aqueous phase was then transferred to another Phase
415 Lock Gel tube. After adding one volume of phenol-chloroform and gentle mixing for 1 min
416 by inversion, centrifugation was performed at 10,000 × g for 10 min at 4°C. The aqueous
417 phase was then transferred to another Phase Lock Gel tube. After adding one volume of
418 chloroform and gentle mixing for 1 min by inversion, centrifugation was performed at 10,000

× g for 10 min at 4°C. The aqueous phase (approximately 300 µl) was recovered in a 1.5 ml tube and DNA was precipitated by adding two volumes of absolute ethanol, 50 µl of sodium acetate (3 M, pH 5.2) and 3 µl of glycogen (5 mg/ml; Invitrogen) as carrier. After incubation on ice for 10 min, the DNA was recovered by centrifugation at 13,000 × g for 30 min at 4°C. The DNA pellet was subsequently washed with 800 µl of 70% (vol/vol) ethanol. After centrifugation at 13,000 × g for 10 min at 4°C, the DNA pellet was dried at room temperature for 30 min and dissolved in 20 µl of 10 mM Tris pH 7.5. Purified DNA was quantified using the Qubit DNA Broad Range assay (ThermoFisher Scientific).

Viral DNA sequencing and bioinformatic analysis

Library preparation and sequencing were performed at the GeT-PlaGe platform (Toulouse, France). Briefly, libraries were prepared using the NEBNext® Ultra™ II DNA Library Prep Kit (New England Biolabs) and sequencing was performed on the MiSeq plateform (Illumina) according to the manufacturer's instructions. Raw reads were quality filtered using Trimmomatic (Bolger et al., 2014) in order to remove paired reads with bad qualities (with length < 125 bp, with remnant of Illumina adapters and with average quality values below Q20 on a sliding window of 4 nt). Furthermore, only the remaining paired reads were kept while those being unpaired at the end of the filtering process were kept aside. The overall filtering process yielded an average of 1.36 million paired-end reads (2 × 250 bp) per sample (2.72 million reads total). All quality-filtered reads from the various experiments were pooled in order to proceed to only one global assembly. Therefore, reads from similar phages but present in several samples would be binned together during the assembly process. Assembly was performed using SPAdes with the *meta* option and increasing *kmer* values -k 21,33,55,77,99,127 (48). Contigs with length below 2,500 bp, unlikely to encode complete viruses, were discarded. The resulting 910 filtered contigs were first analyzed with VirSorter (49), which returned 92 putative viral contigs. A list of “most abundant and pertinent” contigs

was constructed using three criteria: 1) detected as viral with Virsorter, after filtering out those placed in categories 3 or 6 (not so sure) with coverage below 10 (remaining 78 contigs), 2) detected as circular contig, even if not detected as viral (adds 34 contigs) 3) coverage above 100, even if not detected as viral (final list of 124 contigs). These contigs were further analyzed using PHASTER (50) and compared to both the Viruses section of nucleotide database at NCBI and to the complete database using Blast (51) in order to provide a first characterization of putative phage-encoding contigs. Then, quality filtered reads (both paired and unpaired) were mapped individually for each sample against the potential viral contigs using Bowtie2 aligner with default values (52) in order to produce an abundance table. This table was processed with the R package Phyloseq for statistical analysis and data visualization (53). The level of bacterial DNA contamination in the cheese viromes was estimated by detection of ribosomal DNAs among the reads using SortMeRNa software (54) and the SILVA v129 database (55). The three most prevalent contigs present in the final virome, namely Epvir4, 949_Epvir1 and Epvir8, were further annotated using RAST (56). Homologs of the predicted proteins in the contigs were additionally compared to the NCBI nr database using BlastP and HHpred (57) with an E-value cutoff of 10^{-8}.

Accession numbers

Raw sequence data were deposited at the Sequence Read Archive of the National Center for Biotechnology Information under the accession numbers SRR8080803 to SRR8080815 (bioproject PRJNA497596).

ACKNOWLEDGMENTS

This work was conducted in the frame of the Virome Access project supported by the French National Institute for Agricultural Research (INRA) and the Meta-omics and Microbial Ecosystems (MEM) programme. The funders had no role in study design, data collection and

469 interpretation, or the decision to submit the work for publication. We are grateful to Martine
470 and Claude Boccara for their invaluable help with the interferometer device. We thank the
471 INRA GeT-PlaGE platform (https://get.genotoul.fr/la-plateforme/get-plage) for sequencing
472 the Epoisses virome and the INRA MIGALE bioinformatics platform
473 (http://migale.jouy.inra.fr) for providing computational resources and support.

474

475 **REFERENCES**

476 1. Irlinger F, Layec S, Hélinck S, Dugat-Bony E. 2015. Cheese rind microbial communities: diversity,
477 composition and origin. FEMS Microbiol Lett 362:1–11.

478 2. Montel M-C, Buchin S, Mallet A, Delbes-Paus C, Vuitton DA, Desmasures N, Berthier F. 2014.
479 Traditional cheeses: Rich and diverse microbiota with associated benefits. International Journal
480 of Food Microbiology 177:136–154.

481 3. Dugat-Bony E, Garnier L, Denonfoux J, Ferreira S, Sarthou A-S, Bonnarme P, Irlinger F. 2016.
482 Highlighting the microbial diversity of 12 French cheese varieties. International Journal of Food
483 Microbiology 238:265–273.

484 4. Murugesan S, Reyes-Mata MP, Nirmalkar K, Chavez-Carbajal A, Juárez-Hernández JI, Torres-
485 Gómez RE, Piña-Escobedo A, Maya O, Hoyo-Vadillo C, Ramos-Ramírez EG, Salazar-Montoya JA,
486 García-Mena J. 2018. Profiling of bacterial and fungal communities of Mexican cheeses by high
487 throughput DNA sequencing. Food Research International 113:371–381.

488 5. Quigley L, O'Sullivan O, Beresford TP, Ross RP, Fitzgerald GF, Cotter PD. 2012. High-throughput
489 sequencing for detection of subpopulations of bacteria not previously associated with artisanal
490 cheeses. Applied and Environmental Microbiology 78:5717–5723.

491 6. Wolfe BE, Button JE, Santarelli M, Dutton RJ. 2014. Cheese rind communities provide tractable
492 systems for in situ and in vitro studies of microbial diversity. Cell 158:422–433.

493 7. Hyman P, Abedon ST, Hyman P, Abedon ST. 2012. Smaller fleas: viruses of microorganisms.
494 Scientifica 2012:e734023.

495 8. Clokie MRJ, Millard AD, Letarov AV, Heaphy S. 2011. Phages in nature. Bacteriophage 1:31–45.

496 9. Koonin Eugene V., Krupovic Mart, Yutin Natalya. 2015. Evolution of double-stranded DNA
497 viruses of eukaryotes: from bacteriophages to transposons to giant viruses. Annals of the New
498 York Academy of Sciences 1341:10–24.

499 10. La Scola B, Desnues C, Pagnier I, Robert C, Barrassi L, Fournous G, Merchat M, Suzan-Monti M,
500 Forterre P, Koonin E, Raoult D. 2008. The virophage as a unique parasite of the giant mimivirus.
501 Nature 455:100–104.

502 11. de Melo AG, Levesque S, Moineau S. 2018. Phages as friends and enemies in food processing.
503 Current Opinion in Biotechnology 49:185–190.

504 12. Fernández L, Rodríguez A, García P. 2018. Phage or foe: an insight into the impact of viral
505 predation on microbial communities. The ISME Journal 12:1171.

506 13. Sime-Ngando T. 2014. Environmental bacteriophages: viruses of microbes in aquatic
507 ecosystems. Front Microbiol 5:355.

508 14. Park E-J, Kim K-H, Abell GCJ, Kim M-S, Roh SW, Bae J-W. 2011. Metagenomic analysis of the
509 viral communities in fermented foods. Appl Environ Microbiol 77:1284–1291.

510 15. Castro-Mejía JL, Muhammed MK, Kot W, Neve H, Franz CMAP, Hansen LH, Vogensen FK,
511 Nielsen DS. 2015. Optimizing protocols for extraction of bacteriophages prior to metagenomic
512 analyses of phage communities in the human gut. Microbiome 3:64.

513 16. Conceição-Neto N, Zeller M, Lefrère H, Bruyn PD, Beller L, Deboutte W, Yinda CK, Lavigne R,
514 Maes P, Ranst MV, Heylen E, Matthijnssens J. 2015. Modular approach to customise sample

515 preparation procedures for viral metagenomics: a reproducible protocol for virome analysis.
516 Scientific Reports 5:16532.

517 17. Kleiner M, Hooper LV, Duerkop BA. 2015. Evaluation of methods to purify virus-like particles for
518 metagenomic sequencing of intestinal viromes. BMC Genomics 16.

519 18. Thurber RV, Haynes M, Breitbart M, Wegley L, Rohwer F. 2009. Laboratory procedures to
520 generate viral metagenomes. Nature Protocols 4:470–483.

521 19. Stals A, Baert L, Van Coillie E, Uyttendaele M. 2012. Extraction of food-borne viruses from food
522 samples: A review. International Journal of Food Microbiology 153:1–9.

523 20. Biller SJ, McDaniel LD, Breitbart M, Rogers E, Paul JH, Chisholm SW. 2017. Membrane vesicles in
524 sea water: heterogeneous DNA content and implications for viral abundance estimates. The
525 ISME Journal 11:394–404.

526 21. Forterre P, Soler N, Krupovic M, Marguet E, Ackermann H-W. 2013. Fake virus particles
527 generated by fluorescence microscopy. Trends in Microbiology 21:1–5.

528 22. Varsani A, Krupovic M. 2018. Smacoviridae: a new family of animal-associated single-stranded
529 DNA viruses. Arch Virol 163:2005–2015.

530 23. Samson JE, Moineau S. 2010. Characterization of Lactococcus lactis phage 949 and comparison
531 with other lactococcal phages. Appl Environ Microbiol 76:6843–6852.

532 24. Liu Z, Li H, Wang M, Jiang Y, Yang Q, Zhou X, Gong Z, Liu Q, Shao H. 2018. Isolation,
533 characterization and genome sequencing of the novel phage SL25 from the Yellow Sea, China.
534 Marine Genomics 37:31–34.

535 25. Randazzo CL, Torriani S, Akkermans ADL, de Vos WM, Vaughan EE. 2002. Diversity, dynamics,
536 and activity of bacterial communities during production of an artisanal Sicilian cheese as
537 evaluated by 16S rRNA analysis. Appl Environ Microbiol 68:1882–1892.

538 26. Ulve V m., Monnet C, Valence F, Fauquant J, Falentin H, Lortal S. 2008. RNA extraction from
539 cheese for analysis of in situ gene expression of Lactococcus lactis. Journal of Applied
540 Microbiology 105:1327–1333.

541 27. Aherfi S, Colson P, La Scola B, Raoult D. 2016. Giant viruses of amoebas: an update. Front
542 Microbiol 7.

543 28. Roux S, Krupovic M, Debroas D, Forterre P, Enault F. 2013. Assessment of viral community
544 functional potential from viral metagenomes may be hampered by contamination with cellular
545 sequences. Open Biology 3:130160.

546 29. Guo P, El-Gohary Y, Prasadan K, Shiota C, Xiao X, Wiersch J, Paredes J, Tulachan S, Gittes GK.
547 2012. Rapid and simplified purification of recombinant adeno-associated virus. J Virol Methods
548 183:139–146.

549 30. Willner D, Furlan M, Schmieder R, Grasis JA, Pride DT, Relman DA, Angly FE, McDole T, Mariella
550 RP, Rohwer F, Haynes M. 2011. Metagenomic detection of phage-encoded platelet-binding
551 factors in the human oral cavity. PNAS 108:4547–4553.

552 31. Jurczak-Kurek A, Gąsior T, Nejman-Faleńczyk B, Bloch S, Dydecka A, Topka G, Necel A,
553 Jakubowska-Deredas M, Narajczyk M, Richert M, Mieszkowska A, Wróbel B, Węgrzyn G,
554 Węgrzyn A. 2016. Biodiversity of bacteriophages: morphological and biological properties of a
555 large group of phages isolated from urban sewage. Scientific Reports 6:34338.

556 32. Weynberg KD, Wood-Charlson EM, Suttle CA, Oppen V, H MJ. 2014. Generating viral
557 metagenomes from the coral holobiont. Front Microbiol 5.

558 33. Deatherage BL, Cookson BT. 2012. Membrane vesicle release in bacteria, eukaryotes, and
559 archaea: a conserved yet underappreciated aspect of microbial life. Infection and Immunity
560 80:1948–1957.

561 34. Jan AT. 2017. Outer membrane vesicles (OMVs) of gram-negative bacteria: a perspective
562 update. Frontiers in Microbiology 8.

563 35. Toyofuku M, Nomura N, Eberl L. 2018. Types and origins of bacterial membrane vesicles.
564 Nature Reviews Microbiology.

565 36. Reyes-Robles T, Dillard RS, Cairns LS, Silva-Valenzuela CA, Housman M, Ali A, Wright ER, Camilli
566 A. 2018. *Vibrio cholerae* outer membrane vesicles inhibit bacteriophage infection. Journal of
567 Bacteriology 200.

568 37. Yaron S, Kolling GL, Simon L, Matthews KR. 2000. Vesicle-mediated transfer of virulence genes
569 from Escherichia coli O157:H7 to other enteric bacteria. Applied and Environmental
570 Microbiology 66:4414–4420.

571 38. Boccara M, Fedala Y, Bryan CV, Bailly-Bechet M, Bowler C, Boccara AC. 2016. Full-field
572 interferometry for counting and differentiating aquatic biotic nanoparticles: from laboratory to
573 Tara Oceans. Biomed Opt Express 7:3736–3746.

574 39. Roose-Amsaleg C, Fedala Y, Vénien-Bryan C, Garnier J, Boccara A-C, Boccara M. 2017. Utilization
575 of interferometric light microscopy for the rapid analysis of virus abundance in a river. Research
576 in Microbiology 168:413–418.

577 40. Almena-Aliste M, Mietton B. 2014. Cheese classification, characterization, and categorization: a
578 global perspective. Microbiology Spectrum 2.

579 41. McSweeney PLH, Ottogalli G, Fox PF. 2017. Chapter 31 - Diversity and Classification of Cheese
580 Varieties: An Overview, p. 781–808. *In* McSweeney, PLH, Fox, PF, Cotter, PD, Everett, DW (eds.),
581 Cheese (Fourth Edition). Academic Press, San Diego.

582 42. Pinard R, de Winter A, Sarkis GJ, Gerstein MB, Tartaro KR, Plant RN, Egholm M, Rothberg JM,
583 Leamon JH. 2006. Assessment of whole genome amplification-induced bias through high-
584 throughput, massively parallel whole genome sequencing. BMC Genomics 7:216.

585 43. Irlinger F, Mounier J. 2009. Microbial interactions in cheese: implications for cheese quality and
586 safety. Current Opinion in Biotechnology 20:142–148.

587 44. Kastman EK, Kamelamela N, Norville JW, Cosetta CM, Dutton RJ, Wolfe BE. 2016. Biotic
588 interactions shape the ecological distributions of Staphylococcus species. mBio 7:e01157-16.

589 45. Mounier J, Monnet C, Vallaeys T, Arditi R, Sarthou A-S, Helias A, Irlinger F. 2008. Microbial
590 interactions within a cheese microbial community. Applied and Environmental Microbiology
591 74:172–181.

592 46. Zhang Y, Kastman EK, Guasto JS, Wolfe BE. 2018. Fungal networks shape dynamics of bacterial
593 dispersal and community assembly in cheese rind microbiomes. Nature Communications 9:336.

594 47. Schindelin J, Arganda-Carreras I, Frise E, Kaynig V, Longair M, Pietzsch T, Preibisch S, Rueden C,
595 Saalfeld S, Schmid B, Tinevez J-Y, White DJ, Hartenstein V, Eliceiri K, Tomancak P, Cardona A.
596 2012. Fiji: an open-source platform for biological-image analysis. Nature Methods 9:676–682.

597 48. Bankevich A, Nurk S, Antipov D, Gurevich AA, Dvorkin M, Kulikov AS, Lesin VM, Nikolenko SI,
598 Pham S, Prjibelski AD, Pyshkin AV, Sirotkin AV, Vyahhi N, Tesler G, Alekseyev MA, Pevzner PA.
599 2012. SPAdes: a new genome assembly algorithm and its applications to single-cell sequencing.
600 J Comput Biol 19:455–477.

601 49. Roux S, Enault F, Hurwitz BL, Sullivan MB. 2015. VirSorter: mining viral signal from microbial
602 genomic data. PeerJ 3:e985.

603 50. Arndt D, Grant JR, Marcu A, Sajed T, Pon A, Liang Y, Wishart DS. 2016. PHASTER: a better, faster
604 version of the PHAST phage search tool. Nucleic Acids Res 44:W16–W21.

605 51. Altschul SF, Gish W, Miller W, Myers EW, Lipman DJ. 1990. Basic local alignment search tool. J
606 Mol Biol 215:403–410.

607 52. Langmead B, Salzberg SL. 2012. Fast gapped-read alignment with Bowtie 2. Nature Methods
608 9:357–359.

609 53. McMurdie PJ, Holmes S. 2013. phyloseq: an R package for reproducible interactive analysis and
610 graphics of microbiome census data. PLOS ONE 8:e61217.

611 54. Kopylova E, Noé L, Touzet H. 2012. SortMeRNA: fast and accurate filtering of ribosomal RNAs in
612 metatranscriptomic data. Bioinformatics 28:3211–3217.

613 55. Quast C, Pruesse E, Yilmaz P, Gerken J, Schweer T, Yarza P, Peplies J, Glöckner FO. 2013. The
614 SILVA ribosomal RNA gene database project: improved data processing and web-based tools.
615 Nucleic Acids Res 41:D590–D596.

616 56. Aziz RK, Bartels D, Best AA, DeJongh M, Disz T, Edwards RA, Formsma K, Gerdes S, Glass EM,
617 Kubal M, Meyer F, Olsen GJ, Olson R, Osterman AL, Overbeek RA, McNeil LK, Paarmann D,
618 Paczian T, Parrello B, Pusch GD, Reich C, Stevens R, Vassieva O, Vonstein V, Wilke A, Zagnitko O.
619 2008. The RAST Server: rapid annotations using subsystems technology. BMC Genomics 9:75.

620 57. Zimmermann L, Stephens A, Nam S-Z, Rau D, Kübler J, Lozajic M, Gabler F, Söding J, Lupas AN,
621 Alva V. 2018. A completely reimplemented MPI bioinformatics toolkit with a new HHpred
622 server at its core. Journal of Molecular Biology 430:2237–2243.

FIGURE LEGENDS

FIG 1. Schematic representation of the experimental procedure for the extraction of virus-like particles from cheese. The surface of three types of cheese was processed according to four routes named P1 to P4. Steps 1 (homogenization), 2 (centrifugation), 3 (dilution) and 5 (concentration) are common to all protocols, contrary to steps 4 (filtration) and 6 (chloroform treatment) which are optional. For each cheese type, three biological replicates (independent cheeses purchased at the same date and from a unique producer) were performed leading thus to 12 samples per cheese-type.

FIG 2. Photographs of iodixanol density gradients after ultracentrifugation of cheese VLP solutions. Cellular debris and membrane vesicles are concentrated at the top of the 20% iodixanol layer (red arrow) and VLPs at the top of the 45% iodixanol layer (blue arrow). A schematic representation of the gradient is shown on the right. S: sample.

FIG 3. Comparative plot showing the estimated level of bacterial DNA contamination in the Epoisses cheese virome. The expected percentage (x axis) is based on the % of rDNA reads detected by SortMeRNA software. This value was used to calculate the estimated % of bacterial chromosomal DNA using a multiplying factor of (x100) based on estimation that several copies of rRNA operons (*e.g.* 5 copies of ~5 kb in average) would represent about 1% of a bacterial chromosome of an average size of 2.5 Mb. The observed % of possible bacterial contamination was obtained by looking at the % of reads not matching the 124 contigs of the cheese virome. Yellow (P1), red (P2), green (P3), blue (P4) and orange (vesicles sample).

FIG 4. Differences in the Epoisses cheese virome composition according to the VLP extraction procedure. Principal coordinate analysis based on the Bray-Curtis dissimilarity index (A). Relative abundance of the contigs annotated as probable phages (B, 72 contigs), plasmids (C, 19 contigs), putative plasmids (D, 20 contigs), unclassified (E, 14 contigs) and unmapped reads (F).

FIG 5. Heatmap of the 124 contigs composing the Epoisses virome. Samples were grouped according to the VLP extraction procedure. Contigs were separated into four categories (phage, plasmid, putative plasmid and unclassified) according to the annotation results and sorted by abundance inside each group. Yellow to red: lowest to highest relative abundance. Grey: not detected. Ves: vesicles sample.

653 **TABLES**

654 **Table 1.** Quantification of VLPs using interferometry and microbial cells using plate
655 numbering.

Type of Cheese and of protocol	Total nanoparticles (log per g) (SD)	Presence of cells	Presence of noise	Total biomass (log CFU per g) (SD)	Ratio nanoparticles / cell
CAM P1	NA	+++	+++	8.71 (0.11)	NA
EP P1	NA	+++	+++	10.10 (0.31)	NA
SN P1	NA	+++	+++	10.42 (0.07)	NA
CAM P2	10.38 (0.01)	++	-	8.71 (0.11)	47.29 (11.91)
EP P2	10.18 (0.23)	+	-	10.10 (0.31)	1.88 (2.07)
SN P2	10.04 (0.24)	+	-	10.42 (0.07)	0.66 (0.14)
CAM P3	NA	++	+++	8.71 (0.11)	NA
EP P3	NA	-	+++	10.10 (0.31)	NA
SN P3	NA	-	+++	10.42 (0.07)	NA
CAM P4	10.00 (0.13)	-	-	8.71 (0.11)	21.77 (12.15)
EP P4	10.13 (0.37)	-	-	10.10 (0.31)	2.40 (3.35)
SN P4	9.59 (0.40)	-	-	10.42 (0.07)	0.17 (0.10)

656

657 NA: not available because of noise in interferometric measures

SUPPLEMENTARY DATA

Table S1. Microbiological counts obtained for the nine cheese samples.

Table S2. DNA quantities obtained for the different samples studied.

Table S3. Comparison between phage titer and interferometry measure.

Dataset S1. Sequence comparison results of the 124 contigs composing the Epoisses virome.

Dataset S2. Predicted function and best BlastP hit for ORFs of Epvir4 and Epvir8.

Fig. S1. Functional annotation of the three most abundant viral contigs detected in the Epoisses cheese virome. Predicted functions of the ORFs identified in Epvir4 (A), 949_Epvir1 (B) and Epvir8 (C) are color-coded as follow: red for integrase, yellow for transcriptional regulation, orange for replication and recombination, green for DNA packaging and head, light blue for connector, dark blue for tail, light pink for homing endonuclease, dark pink for lysis, grey for hypothetical proteins, violet for additional functions. Some of the predicted functions of the ORFs are detailed for each contig.

Fig. S2. Comparison between phage concentration as measured by titration and using the interferometric light microscope (ILM). Six reference phages were used for the comparison, namely phages P1, T4, T5, T7, λCI857 and φX174.

Fig. S3. Epifluorescence image of a VLP solution obtained from Epoisses cheese. The VLP solution was diluted 10-fold in 1 ml of SM buffer with gluteraldehyde (2.5% final), incubated 10 minutes on ice and then flash frozen in liquid nitrogen. 100 µl of the nanoparticle solution was diluted into 5 ml of filtered water; and then filtered through a 25 mm anodisc membrane with pore sizes of 0.02 µm and stained with 100 µL of SYBR Gold (50×) for 15 min in the dark. Filters were placed on a microscopy slide with 100 µL of anti-fading solution Fluoromount, and observed immediately after preparation on a microscope Leica DMRA2 microscope equipped with a × 100 magnification oil-immersion objective and a COOLSNAP

682 HQ camera (Roper Scientific, USA), using YFP filters. Images were captured and processed

683 with METAMORPH V6.3r5.

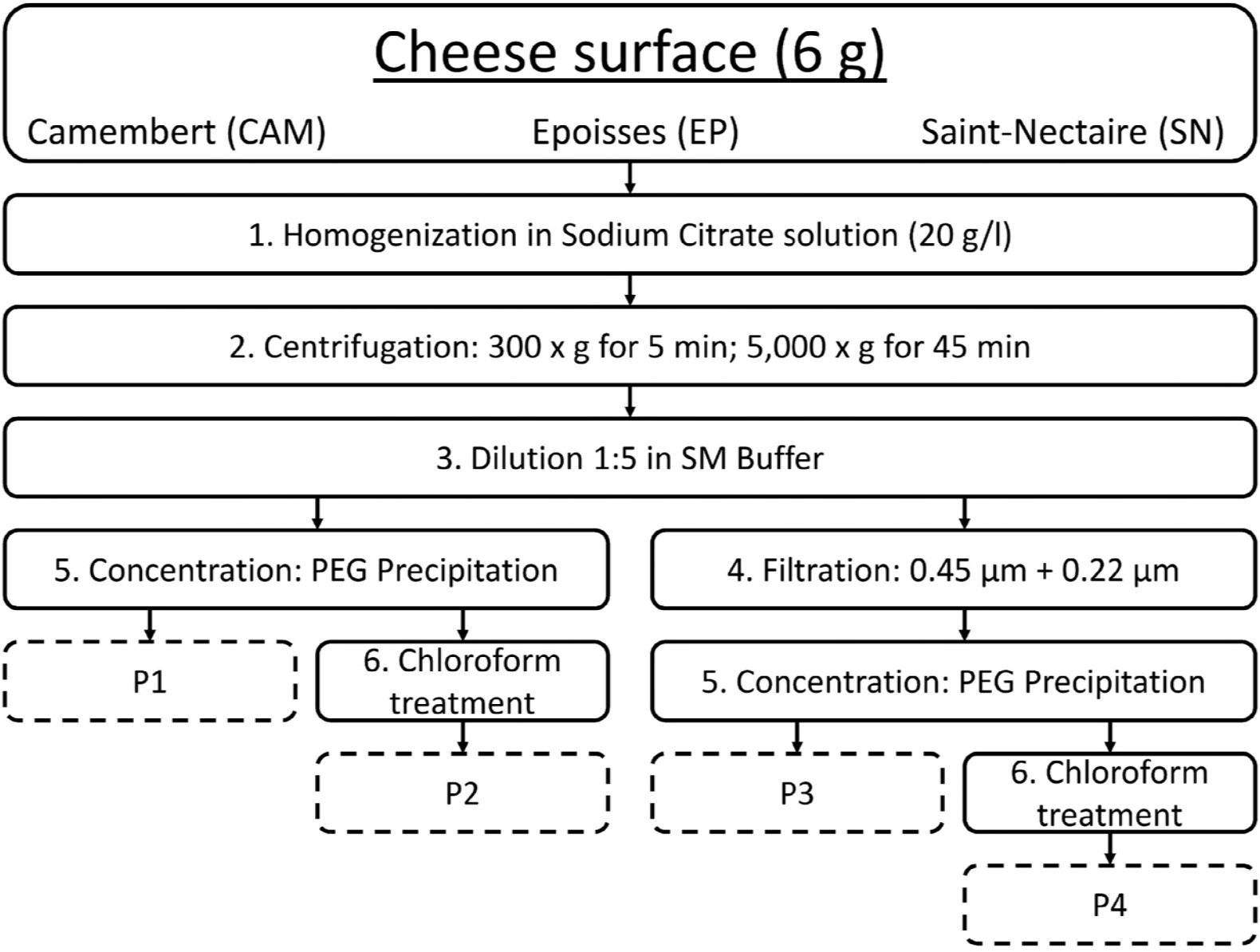
Cheese surface (6 g)
Camembert (CAM)
Epoisses (EP)
Saint-Nectaire (SN)
1. Homogenization in Sodium Citrate solution (20 g/l)
2. Centrifugation: 300 x g for 5 min; 5,000 x g for 45 min
3. Dilution 1:5 in SM Buffer
5. Concentration: PEG Precipitation
4. Filtration: 0.45 µm + 0.22 µm
P1
6. Chloroform treatment
5. Concentration: PEG Precipitation
P2
P3
6. Chloroform treatment
P4

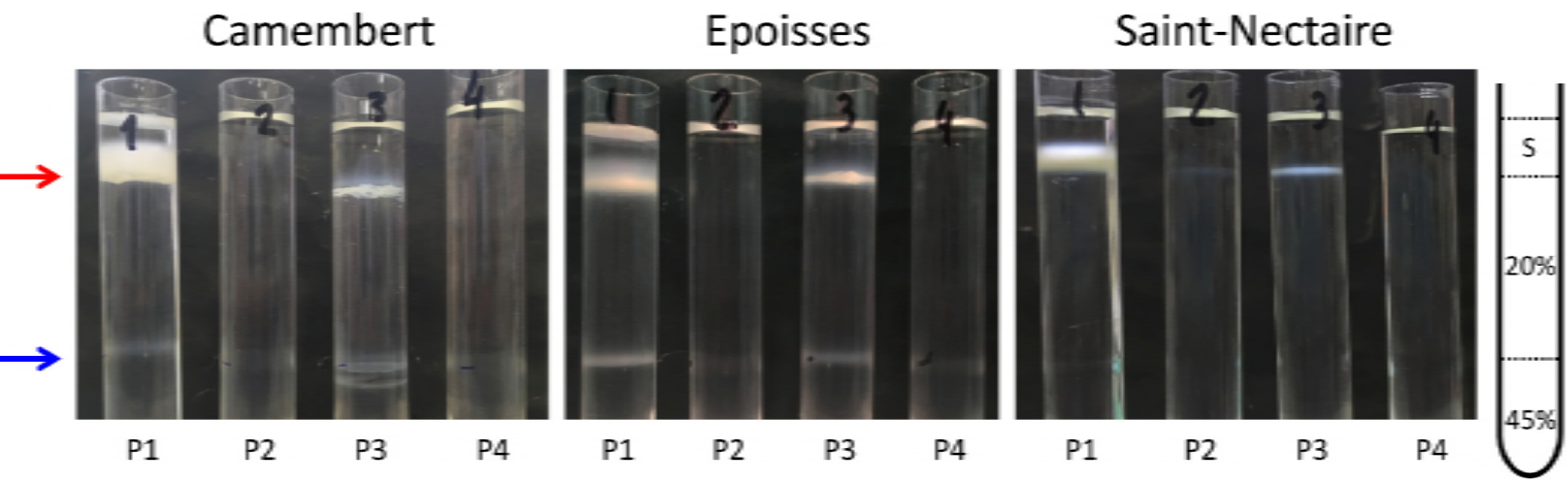
Camembert
Epoisses
Saint-Nectaire
1
2
3
4
S
20%
45%
P1
P2
P3
P4
P1
P2
P3
P4
P1
P2
P3
P4

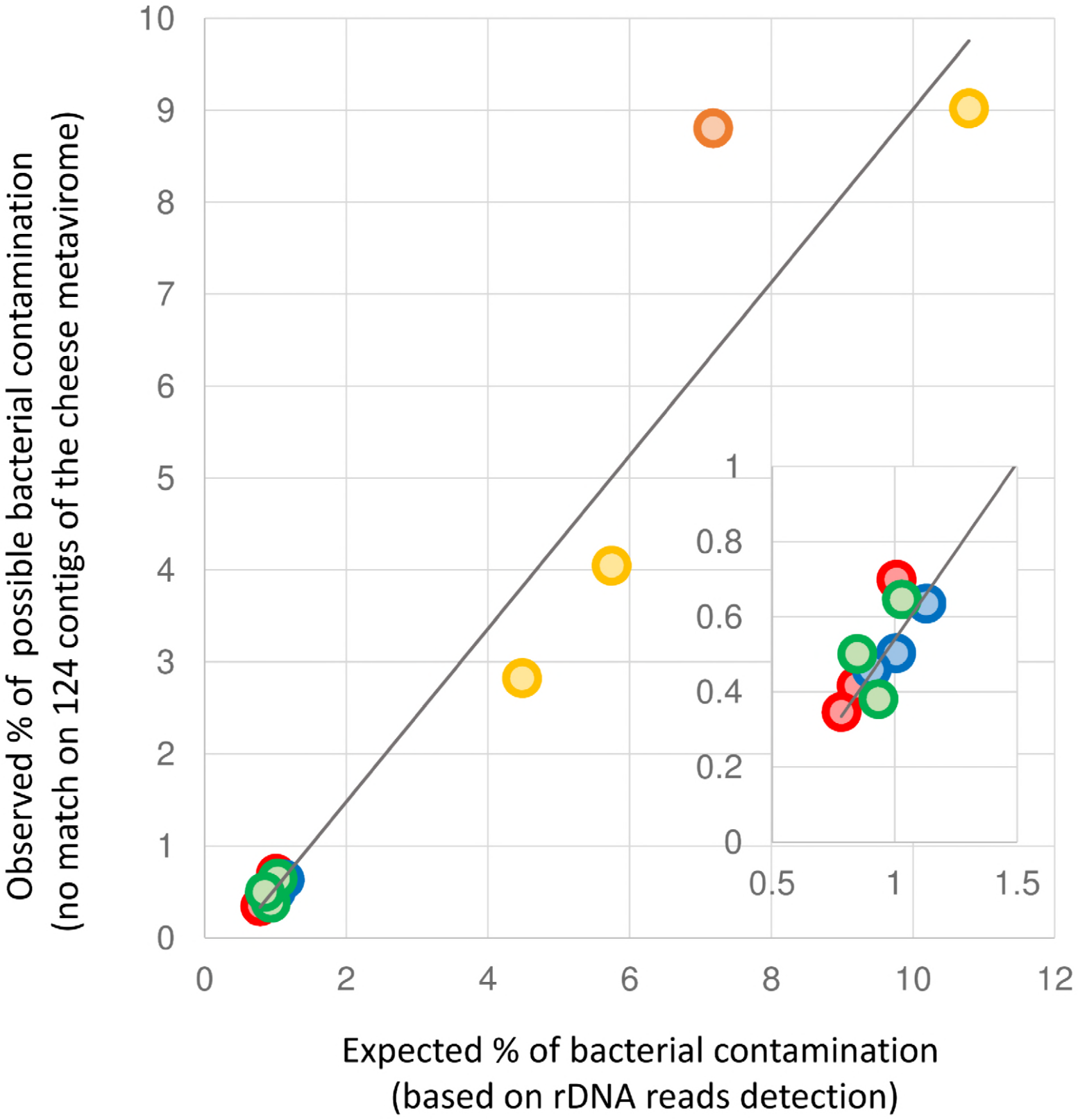
Observed % of possible bacterial contamination
(no match on 124 contigs of the cheese metavirome)
Expected % of bacterial contamination
(based on rDNA reads detection)
0
1
2
3
4
5
6
7
8
9
10
0
2
4
6
8
10
12
0
0.2
0.4
0.6
0.8
1
0.5
1
1.5

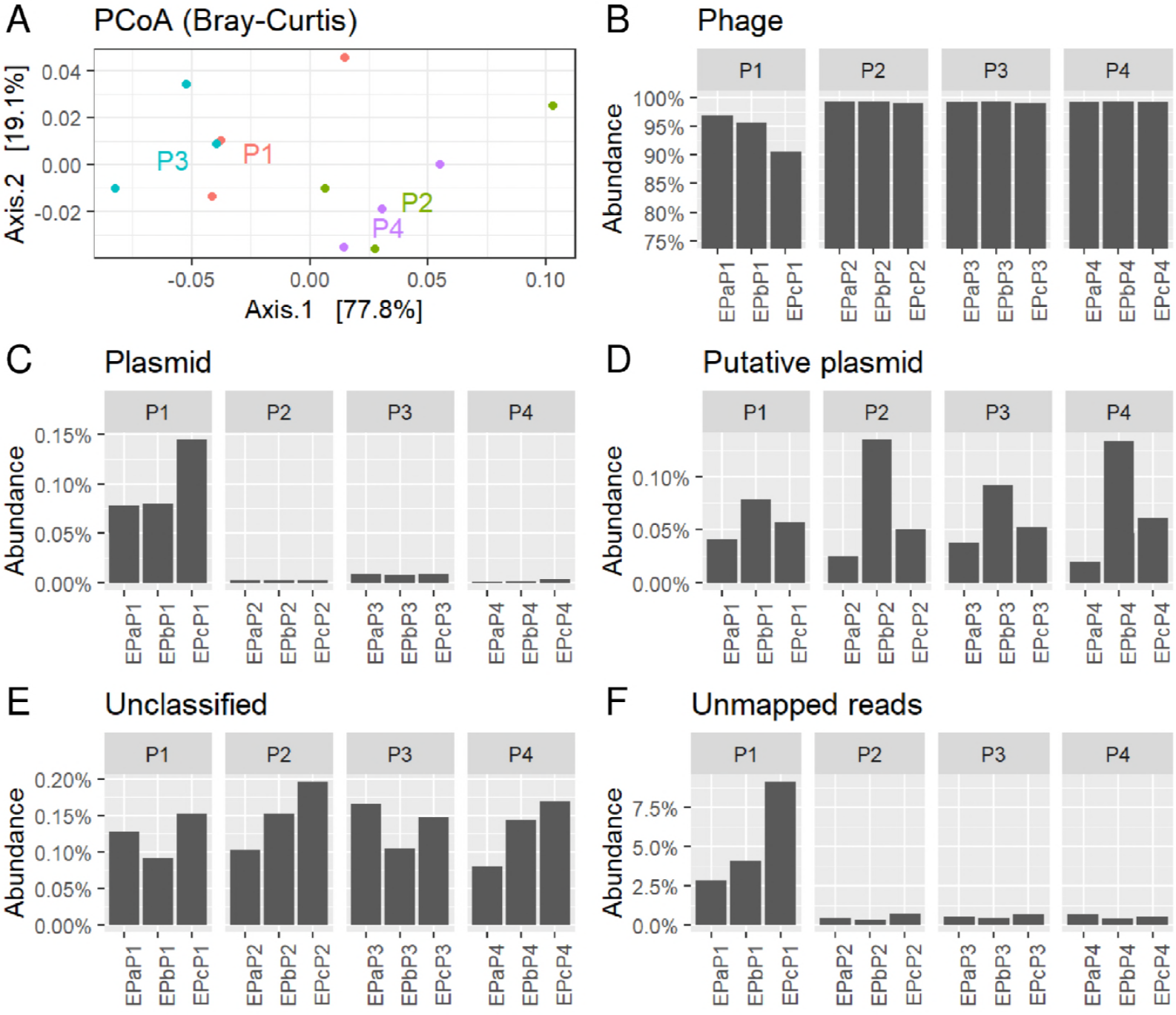
A
PCoA (Bray-Curtis)
Axis.2 [19.1%]
Axis.1 [77.8%]
P1
P2
P3
P4
B
Phage
Abundance
C
Plasmid
D
Putative plasmid
E
Unclassified
F
Unmapped reads
EPaP1
EPbP1
EPcP1
EPaP2
EPbP2
EPcP2
EPaP3
EPbP3
EPcP3
EPaP4
EPbP4
EPcP4

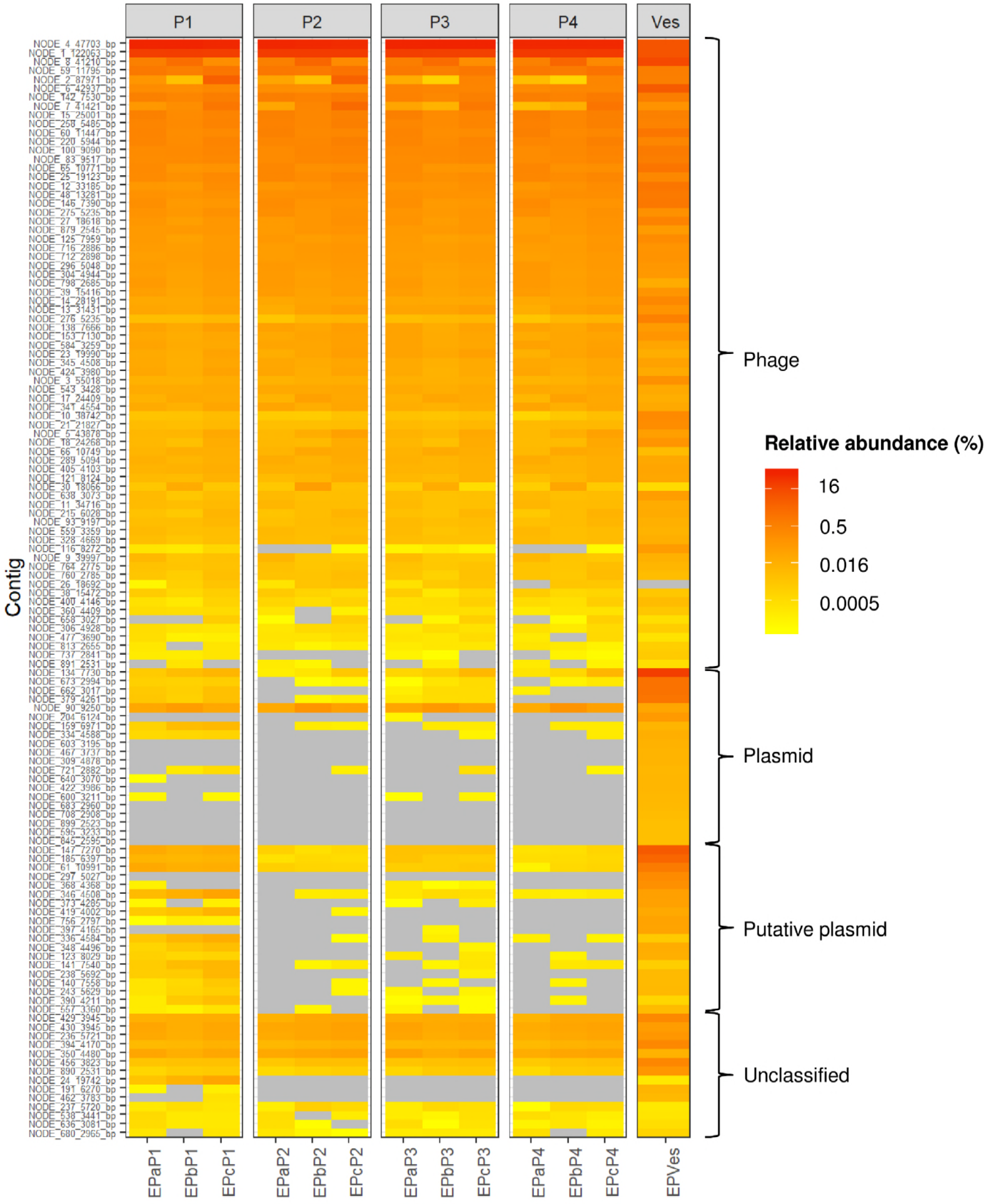
P1
P2
P3
P4
Ves
Contig
NODE_4_47703_bp
NODE_1_122063_bp
NODE_8_41210_bp
NODE_59_11795_bp
NODE_2_87971_bp
NODE_6_42937_bp
NODE_142_7530_bp
NODE_7_41421_bp
NODE_15_25001_bp
NODE_258_5486_bp
NODE_60_11447_bp
NODE_220_5944_bp
NODE_100_9090_bp
NODE_83_9517_bp
NODE_55_10771_bp
NODE_25_19123_bp
NODE_12_33186_bp
NODE_48_13281_bp
NODE_145_7390_bp
NODE_275_5235_bp
NODE_27_18618_bp
NODE_879_2545_bp
NODE_125_7959_bp
NODE_716_2886_bp
NODE_712_2898_bp
NODE_296_5048_bp
NODE_304_4944_bp
NODE_798_2685_bp
NODE_39_15416_bp
NODE_14_28191_bp
NODE_13_31431_bp
NODE_276_5235_bp
NODE_138_7666_bp
NODE_153_7130_bp
NODE_584_3259_bp
NODE_23_19990_bp
NODE_345_4508_bp
NODE_424_3980_bp
NODE_3_55018_bp
NODE_543_3428_bp
NODE_17_24409_bp
NODE_341_4554_bp
NODE_10_38742_bp
NODE_21_21827_bp
NODE_5_43878_bp
NODE_18_24268_bp
NODE_66_10749_bp
NODE_289_5094_bp
NODE_405_4103_bp
NODE_121_8124_bp
NODE_30_18066_bp
NODE_638_3073_bp
NODE_11_34716_bp
NODE_215_6026_bp
NODE_93_9197_bp
NODE_559_3359_bp
NODE_328_4669_bp
NODE_116_8272_bp
NODE_9_39997_bp
NODE_764_2775_bp
NODE_760_2785_bp
NODE_26_18692_bp
NODE_38_15472_bp
NODE_400_4146_bp
NODE_360_4409_bp
NODE_658_3027_bp
NODE_306_4928_bp
NODE_477_3690_bp
NODE_813_2655_bp
NODE_737_2841_bp
NODE_891_2531_bp
NODE_134_7730_bp
NODE_673_2994_bp
NODE_662_3017_bp
NODE_379_4261_bp
NODE_90_9250_bp
NODE_204_6124_bp
NODE_159_6971_bp
NODE_334_4588_bp
NODE_603_3195_bp
NODE_467_3737_bp
NODE_309_4878_bp
NODE_721_2882_bp
NODE_640_3070_bp
NODE_422_3986_bp
NODE_600_3211_bp
NODE_683_2960_bp
NODE_708_2908_bp
NODE_899_2523_bp
NODE_595_3233_bp
NODE_645_2595_bp
NODE_147_7270_bp
NODE_185_6397_bp
NODE_61_10991_bp
NODE_297_5027_bp
NODE_368_4368_bp
NODE_346_4508_bp
NODE_373_4285_bp
NODE_419_4002_bp
NODE_756_2797_bp
NODE_397_4165_bp
NODE_336_4584_bp
NODE_348_4496_bp
NODE_123_8029_bp
NODE_141_7540_bp
NODE_238_5692_bp
NODE_140_7558_bp
NODE_243_5629_bp
NODE_390_4211_bp
NODE_557_3360_bp
NODE_429_3945_bp
NODE_430_3945_bp
NODE_236_5721_bp
NODE_394_4170_bp
NODE_350_4480_bp
NODE_456_3823_bp
NODE_890_2531_bp
NODE_24_19742_bp
NODE_191_6270_bp
NODE_462_3783_bp
NODE_237_5720_bp
NODE_538_3441_bp
NODE_636_3081_bp
NODE_680_2965_bp
EPaP1
EPbP1
EPcP1
EPaP2
EPbP2
EPcP2
EPaP3
EPbP3
EPcP3
EPaP4
EPbP4
EPcP4
EPVes
Phage
Plasmid
Putative plasmid
Unclassified
Relative abundance (%)
16
0.5
0.016
0.0005